Enhanced spontaneous emission from semiconductor nanocrystals embedded in whispering gallery optical microcavities

Xudong Fan,[1] Mark C. Lonergan,[2] Yuzhong Zhang,[3] and Hailin Wang[1]
[1]*Department of Physics, University of Oregon, Eugene, Oregon 97403*
[2]*Department of Chemistry, University of Oregon, Eugene, Oregon 97403*
[3]*Molecular Probes, Inc., Eugene, Oregon 97402*
(Received 1 March 2001; published 27 August 2001)

Cavity-QED studies in a low-Q regime demonstrate enhanced spontaneous emission from CdSe/ZnS core/shell nanocrystals embedded in a polystyrene microsphere and provide important information on radiative dynamics in these quantum dots. The cavity-induced relative enhancement in photoluminescence decay rates depends sensitively on the relative contribution of radiative and nonradiative decay processes. The experimental results, including the temperature and nanocrystal size dependence of the time-resolved photoluminescence, suggest that the enhanced spontaneous emission arises from photoluminescence from the lowest dipole-allowed transition. For large nanocrystals, decay of the transition is primarily radiative in origin.

DOI: 10.1103/PhysRevB.64.115310 PACS number(s): 78.67.Bf, 42.50.−p, 78.66.−w

Spontaneous-emission-reflecting optical interactions between matter and vacuum can be controlled by using optical microcavities. Extensive experimental efforts using composite atom-cavity systems have led to the achievement of the strong-coupling regime where the dipole-coupling rate between a single atom and a resonant-cavity mode exceeds both the atomic-dephasing rate and the cavity-decay rate.[1] Optical processes including reversible spontaneous emission in this regime have been successfully exploited to explore a variety of topics such as quantum measurement, entanglement, and more recently quantum information processing.[1,2] The progress made in atomic cavity QED (CQED) has further stimulated considerable interest in CQED of quantum dots (QD's) that feature atomiclike discrete energy levels.[3] In addition to applications such as microlasers, composite QD-cavity systems avoid the difficulty of center-of-mass motion inherent in atomic CQED and can, in principle, scale up to a relatively large mesoscopic system, for example, having an array of QD's couple strongly to a cavity mode.

Experimental efforts toward achieving the strong-coupling regime using monolithic QD-microcavity systems have thus far been hindered by the inadequate cavity finesse and by rapid dephasing in QD's. To overcome these difficulties, we have proposed to use a composite QD-microcavity system where colloidal QD's or semiconductor nanocrystals couple to a whispering-gallery mode (WGM) in a fused-silica microsphere.[4] The composite system features a cavity finesse two orders of magnitude greater than that of monolithic semiconductor microcavities. Compared with QD's grown by molecular-beam epitaxy (MBE), colloidal QD's are characterized by completely quantized acoustic phonon modes, which can suppress dephasing associated with electron-phonon interactions. Homogeneous linewidth of order 30 μeV has been recently observed in CdSe nanocrystals, compared with a homogeneous linewidth of order 1 meV in the absence of phonon quantization.[5] Homogeneous linewidth of order 1 μeV, more than one order of magnitude smaller than that observed in any QD system grown by MBE, has also been achieved in CuCl nanocrystals embedded in a NaCl crystal.[6]

Whether optical interactions in colloidal QD's such as CdSe nanocrystals can be controlled with an optical microcavity, however, remains an open question. In spite of many recent advances, radiative dynamics, especially the physical nature of band-edge photoluminescence (PL), in colloidal QD's is still not well understood. Time-resolved PL from these nanocrystals features multiple decay components with decay times ranging from μs to ns. This along with the complex energy structure near the band edge of the colloidal QD's makes it difficult to extract information on the underlying decay processes. To be able to control optical interactions in a QD with an optical microcavity, it is important that the relevant dynamics be dominated by radiative instead of nonradiative decay processes.

In this paper we report experimental studies that have enabled us to probe radiative dynamics in CdSe nanocrystals and to demonstrate the feasibility of controlling radiative dynamics in these QD's with whispering-gallery optical microcavities. The experimental approach is based on CQED in a low-Q regime. In this regime, the enhancement in the spontaneous emission or the radiative decay rate is characterized by the Purcell factor given by $F_p=\Gamma_c/\Gamma_r$ where Γ_c is the radiative decay rate into a cavity mode and Γ_r is the radiative decay rate in a homogeneous dielectric medium.[7] The cavity-induced relative change in the total decay rate $\Gamma_t=\Gamma_{\mathrm{nonr}}+\Gamma_r$, where Γ_{nonr} is the nonradiative decay rate, depends on the relative contribution of Γ_r and Γ_{nonr} and is given by

$$\varepsilon=\frac{\Gamma_{\mathrm{nonr}}+(1+F_p)\Gamma_r}{\Gamma_{\mathrm{nonr}}+\Gamma_r}-1=F_p\frac{1}{1+\Gamma_{\mathrm{nonr}}/\Gamma_r}. \qquad (1)$$

since Γ_{nonr} is not affected by the cavity. The manifestation of CQED effects thus depends sensitively on the ratio $\Gamma_{\mathrm{nonr}}/\Gamma_r$, providing information on the underlying radiative dynamics that is otherwise not available from conventional time-resolved PL studies. For large nanocrystals ($R\sim 4.5$ nm), ε approaches the theoretically expected F_p, indicating that decay of the underlying optical transition is primarily radiative in origin. These studies represent a crucial first step toward the use of colloidal QD's to achieve the

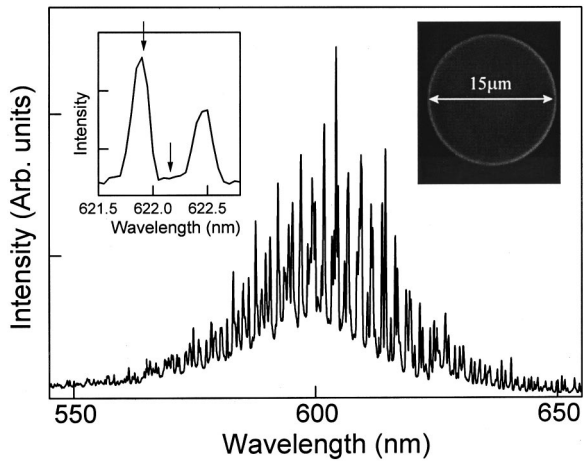

FIG. 1. PL spectrum from nanocrystals with $R=2.7$ nm, embedded in the interior surface of a polystyrene sphere. The bright ring in the right inset is due to PL from embedded nanocrystals. Arrows in the left inset indicate the spectral positions used for the time-resolved PL in Fig. 3.

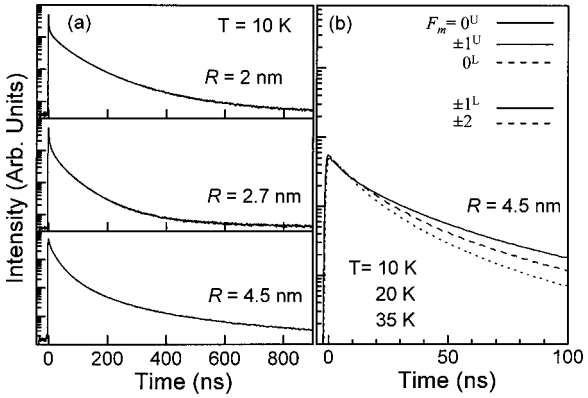

FIG. 2. Time-resolved PL from nanocrystals in free space. (a) At 10 K. (b) Temperature dependence. Solid, dashed, and dotted curves are obtained at 10, 20, and 35 K, respectively, with the amplitude normalized to the same peak intensity. The inset in (b) shows schematically the excitonic-energy structure near the band edge.

strong-coupling regime and furthermore provide the much needed information on radiative dynamics that is essential for understanding optical properties in these remarkable QD's.

CdSe/ZnS core/shell nanocrystals used in our study were fabricated by using a high-temperature organometallic synthesis developed earlier.[8] In these nanocrystals, a CdSe core is capped by a thin shell of ZnS with a band gap greater than that of CdSe. The ZnS shell significantly improves the quantum yield of the nanocrystals with an average room-temperature quantum yield of 40–50 %.[8] Three groups of nanocrystals with average core radius R of 2, 2.7, and 4.5 nm (referred to as NC1, NC2, and NC3, respectively) were used. The average core radii were determined from PL spectra and are consistent with results of transmission-electron microscopy. For CQED studies, CdSe/ZnS nanocrystals were doped in the interior surface of a polystyrene sphere.[9] No indications of degradation due to the doping process have been observed. An inset in Fig. 1 shows the optical image of a typical nanocrystal-doped polystyrene sphere.

Dielectric spheres are versatile optical cavities.[10,11] In these spheres, WGM's form via total internal reflection. Lowest-order WGM's propagate along an equatorial ring of the sphere surface. For studies presented in this paper, polystyrene spheres with a diameter of 15 μm were used. Separate control experiments also used spheres with a diameter of 100 μm (no CQED effects were observed with these spheres). Figure 1 shows the PL spectrum obtained at 10 K from NC2 embedded in a polystyrene sphere. A SPEX-750M spectrometer with a spectral resolution of 0.02 nm is used. The linewidth of the narrowest WGM's as shown in the inset, is 0.2 nm, corresponding to a Q factor of 3000. Note that for the purpose discussed above, only a modest F_p is needed. Hence, we have chosen to use polystyrene spheres instead of fused-silica microspheres that feature much greater Q factors. Using a high-Q fused-silica-microsphere system for studies of enhanced spontaneous-emission rates also means that the time-resolved study needs to be performed with a spectral resolution better than 0.01 nm, which is very difficult to achieve.

Assuming that optical dipoles are randomly orientated, resonant with the cavity mode, and positioned at the maximum of the vacuum electric field, and that the homogeneous linewidth of the transition is smaller than the cavity linewidth, we have $F_p=QD\lambda^3/4\pi^2n^3V$, where n is the index of the sphere, λ is the wavelength in vacuum, D is the mode degeneracy, and V is the effective mode volume defined as the spatial integral of the field intensity, normalized to unity at the maximum.[7,10] For a 15-μm sphere, using $Q=3000$, $\lambda=620$ nm, $n=1.5$, $D=2$, and $V=35\,\mu\mathrm{m}^3$ for the WGM's we obtain $F_p=0.3$. The actual effective Purcell factor is smaller due to the spatial and spectral distributions of nanocrystals in the measurement. Using statistical average similar to that used in Ref. 12, we obtain an effective Purcell factor of 0.2.

Time-resolved PL was carried out by using correlated photon counting. The excitation pulses, obtained by frequency-doubling a mode-locked Ti:Sapphire laser, were centered near $\lambda=400$ nm with a reduced repetition rate of 500 kHz. A photomultiplier tube was used as the detector with a system response near 1.5 ns. Experimental results presented were obtained at excitation levels where behaviors of time-resolved PL are independent of the input pulse energy.

Figure 2(a) shows time-resolved PL in free space. Qualitatively the same results have also been obtained by using CdSe/ZnS core/shell nanocrystals from another group.[13] At 10 K decay times of PL range from of the order of 1 ns to a few hundred nanoseconds. This complex behavior of multiple decay components is in part due to the exciton-energy structure in nanocrystals. The energy structure of band-edge excitons in CdSe nanocrystals, drawn schematically in the inset of Fig. 2(b) is characterized by five levels with angular momentum projection $F_m=\pm2$, $\pm1^L$, $0^L\pm1^U$, 0^U, where U and L denote upper and lower states with the same F_m.[14] Within the effective-mass approximation (EMA), transitions from the crystal ground state to states ±2 and 0^L (dashed

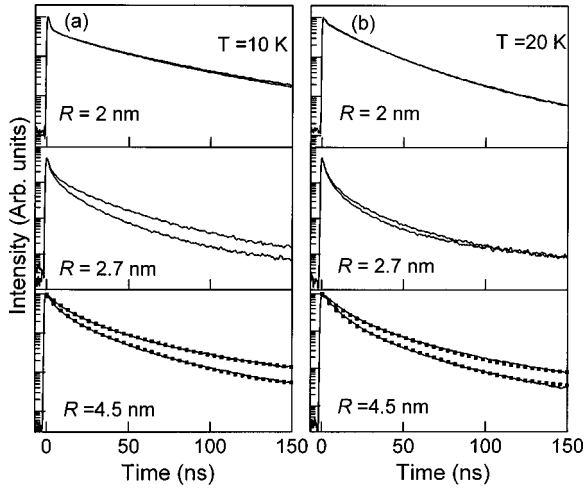

FIG. 3. Time-resolved PL from nanocrystals embedded in a polystyrene sphere at spectral positions, resonant (the lower curve in each figure) or off resonant (the upper curve in each figure) with given WGM's. The measurements were carried out at the lower-energy side of the respective PL spectra. For each figure, the amplitude is normalized to the same peak intensity. (a) At 10 K. (b) At 20 K. Results of numerical fits to PL from nanocrystals with $R = 4.5$ nm are shown as squares and are discussed in the text.

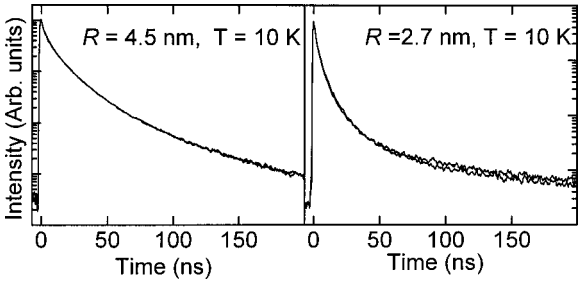

FIG. 4. Time-resolved PL from nanocrystals embedded in a polystyrene sphere obtained near the center of the respective PL spectra and with the amplitude normalized to the same peak intensity. Results obtained at a wavelength resonant with a given WGM and at a nearby wavelength, but off resonant with the WGM, are shown in each figure and are nearly the same.

lines) are dipole forbidden, while transitions to states $\pm 1^L$, $\pm 1^U$, and 0^U (solid lines) are dipole allowed. In addition to direct radiative recombination, phonon-assisted optical transitions from both dipole-allowed and dipole-forbidden transitions can also contribute to the PL.[14]

For a collection of nanocrystals with a large inhomogeneous linewidth, a number of direct as well as phonon-assisted optical transitions can contribute to PL measured at a given wavelength. In principle, each transition can lead to a single or multiple decay components in the time-resolved PL with the decay including both radiative and nonradiative processes. In order to reduce contributions from higher excited states, time-resolved PL presented in this paper was obtained at the lower-energy end of the PL spectrum unless otherwise specified. Little information on details of the underlying radiative dynamics, however, can be extracted from the conventional time-resolved PL since it is difficult to correlate decay components with a specific optical transition.

Figure 3 shows time-resolved PL of nanocrystals embedded in polystyrene spheres. In each part, the lower curve is obtained at a wavelength resonant with a WGM while the upper curve is obtained at a wavelength near but is off resonant ($\sim$3 Å away) with the given WGM. For these measurements, a spectral bandwidth of 1 Å was used in order to separate the resonant and off-resonant contributions. Because of this, the signal level is relatively low with counts per second of the order of 100. Data-acquisition time of the order of 1 h is typically needed in order to obtain a good signal-to-noise ratio for a time-resolved PL curve. Note that in free space, behaviors of time-resolved PL within a narrow spectral range of 5 Å are nearly identical. An example of the relevant wavelength positions is also shown in the inset in Fig. 1. As shown in Fig. 3, the enhancement in PL decay rates when the PL is resonant with a given WGM occurs for only one PL component and the relative enhancement depends sensitively on temperature and especially nanocrystal sizes.

To understand the manifestation of CQED effects, we emphasize that as long as the homogeneous linewidth is small compared with the cavity linewidth, F_p is determined by the properties of the cavity and remains nearly the same for all measurements in Fig. 3.[12] For a relatively small $F_p(\sim 0.2)$, clear signature of relative changes in the total decay rate can be observed only when Γ_r is greater than or at least comparable to Γ_{nonr}, as indicated by Eq. (1).

We attribute the PL component that exhibits pronounced cavity-induced enhancement in the decay rate to optical emissions from states $\pm 1^L$, the lowest dipole-allowed transition. For these states, Γ_{nonr} includes contributions from thermal activation to higher excited states, decay to states ± 2, and possibly relaxation to surface states. The decay into the ± 2 states requires spin flipping of excitations, which is shown to be extremely slow in recent studies using time-resolved Faraday rotation.[15] At low temperature, thermal activation from the $\pm 1^L$ to $\pm 1^U$ states is also slow because of the large energy separation (>10 meV) between these states.[14] In comparison, for dipole-allowed transitions with energies higher than the $\pm 1^L$ states, rapid relaxation into lower-energy states are expected since in this case the relaxation does not require spin flipping. Hence, for these higher excited states, Γ_{nonr} is much greater than Γ_r. PL from these states should contribute to the initial fast-decay component in time-resolved PL. No significant cavity-induced relative increase in the decay rates, however, is expected for PL from these higher excited states. We also note that for all nanocrystals we have used, no pronounced enhancement in PL decay rates was observed for PL obtained at the center (see Fig. 4) or at the higher-energy side of the PL spectra where contributions from higher excited states become much more important.

The above assignment on the PL from the lowest dipole-allowed transition is further supported by the size and the temperature dependence of the CQED effects shown in Fig. 3. The enhancement in PL decay rates can only be observed

in relatively large nanocrystals (NC2 and NC3 but not NC1). Earlier theoretical calculations have shown that the relative oscillator strength for the $\pm 1^L$ states increases with increasing nanocrystal size.[14,16] On the other hand, the relative oscillator strength for the $\pm 1^U$ states decreases with increasing nanocrystal size. When the nanocrystal size decreases from more than 3 to 1.5 nm in radius, radiative lifetime $1/\Gamma_r$ for the $\pm 1^L$ states increases from 10 to 100 ns. The ratio $\Gamma_r/\Gamma_{\text{nonr}}$ for the $\pm 1^L$ states is thus expected to decrease with decreasing nanocrystal size. Hence, smaller nanocrystals should feature a smaller ε as well as a smaller relative contribution from the $\pm 1^L$ states to the overall PL, leading to negligible CQED effects as observed for NC1.

Figure 3 also shows that at low temperature, ε for NC3 exhibits only a weak temperature dependence, in agreement with the weak temperature dependence of the time-resolved PL (within the first 20 ns) obtained in free space, as shown in Fig. 2(b). In comparison, much stronger temperature dependence of ε is observed for NC2. This size variation in the temperature dependence of ε is expected since as we discussed above, smaller nanocrystals feature a smaller ratio of $\Gamma_r/\Gamma_{\text{nonr}}$. For these nanocrystals, ε is more strongly affected by the temperature dependence in Γ_{nonr}.

For a quantitative analysis, we have focused on results obtained for NC3 and have used two exponential components to fit the PL in the first 150 ns (numerical analysis of results on NC2 and NC1 are more involved due to the presence of an initial fast-decay component). For nanocrystals off resonant with the relevant WGM, the decay time for the first decay component is $1/\Gamma_t = 8.7$ and 8.1 ns at 10 and 20 K, respectively (the decay time for the second and slower component is of the order of 30 ns at 10 K). Whereas for nanocrystals resonant with the relevant WGM, the decay time for the first decay component is $1/\Gamma_t = 7.3$ and 6.8 ns at 10 and 20 K, respectively. These results yield $\varepsilon = 0.2$ and 0.19 at 10 and 20 K, respectively, approaching the theoretically expected F_p and thus indicating that the underlying decay process is primarily radiative in origin. For very large nanocrystals, radiative decay time $(1/\Gamma_r)$ for the lowest dipole-allowed transition is theoretically expected to be of the order of 10 ns, in general agreement with the experimental result.[16] Note that although there are considerable error bars ($\pm 20\%$) in the numerical analysis, the observation of the pronounced cavity-induced enhancement in the total decay rate by itself indicates that Γ_r is considerably greater than Γ_{nonr} since otherwise ε would be too small to have a significant effect, as shown by Eq. (1). This is further supported by the weak temperature dependence in both ε and Γ_t discussed above. Hence, for large nanocrystals, population decay of the lowest dipole-allowed transition is primarily radiative in origin in spite of the complex energy structure and relaxation processes, which is important for the use of these QD's for cavity QED in the strong-coupling regime.

In summary, experimental studies of CQED effects in a low-Q regime have enabled us to obtain important and much needed information on radiative dynamics in semiconductor nanocrystals and to demonstrate the feasibility of controlling optical interactions in these QD's with whispering-gallery optical microcavities. The cavity-induced relative enhancement in PL decay rates depends sensitively on the relative contribution of radiative and nonradiative decay processes. The experimental results, including the temperature and the nanocrystal size dependence of the time-resolved photoluminescence, suggest that the enhanced spontaneous emission arises from the lowest dipole-allowed transition in CdSe nanocrystals. For large nanocrystals ($R \sim 4.5$ nm), decay of the transition is primarily radiative in origin. These results, along with earlier results on both the dephasing rate and the cavity finesse of a composite nanocrystal-fused-silica-microsphere system, indicate that this composite system is highly promising toward reaching the strong-coupling regime for QD's thus opening up a new frontier toward manipulating and controlling optical interactions in mesoscopic quantum systems.

H.W. thanks Al. L. Efros for helpful and stimulating discussions. We also thank P.C. Sercel for the use of the correlated photon-counting system. This work was supported by NSF Grant No. DMR-9733230.

[1] For a review, see *Cavity Quantum Electrodynamics*, edited by P. R. Berman (Academic, Boston, 1994).

[2] For recent development, see, for example, C. J. Hood, T. W. Lynn, A. C. Doherty, A. S. Papkins, and H. J. Kimble, Science **287**, 1447 (2000); G. Noques, A. Rauschenbeutel, S. Osnaghi, N. Brune, J. M. Raimond, and S. Haroche, Nature (London) **400**, 239 (1999).

[3] For an earlier review, see Y. Yamamoto and R. E. Slusher, Phys. Today **46(6)**, 66 (1993).

[4] X. Fan, S. Lacey, P. Palinginis, H. Wang, and M. Lonergan, Opt. Lett. **25**, 1600 (2000).

[5] P. Palinginis and H. Wang, Appl. Phys. Lett. **78**, 1541 (2001); K. Takemoto, B. R. Hyun, and Y. Masumoto, Solid State Commun. **114**, 521 (2000).

[6] M. Ikezawa and Y. Masumoto, Phys. Rev. B **61**, 12 662 (2000).

[7] E. M. Purcell, Phys. Rev. **69**, 681 (1946).

[8] M. A. Hines and P. Guyot-Sionnest, J. Phys. Chem. **100**, 468 (1995).

[9] Nanocrystals have also been doped in other polymer spheres, see M. V. Artemyev and U. Woggon, Appl. Phys. Lett. **76**, 1353 (2000).

[10] For a review, see, for example, *Optical processes in microcavities*, edited by R. K. Chang and A. J. Campillo (World Scientific, Singapore, 1996). For discussions on enhanced spontaneous emission in molecular fluorescence, see, for example, P. R. Chance, A. Prock, and R. Silbey, in *Advances in Chemical Physics*, edited by I. Prigogine and S. A. Rice (Wiley, New York, 1978), Vol. 37, p. 1.

[11] V. B. Braginsky, M. L. Gorodetsky, and V. S. Ilchenko, Phys. Lett. A **137**, 393 (1989).

[12] J. M. Gérard, B. Sermage, B. Gayral, B. Legrand, E. Costard, and V. Thierry-Meig, Phys. Rev. Lett. **81**, 1110 (1998).
[13] Weidong Yang and A. P. Alivisatos (unpulished).
[14] Al. L. Efros, M. Rosen, M. Kuno, M. Nirmal, D. J. Norris, and M. Bawendi, Phys. Rev. B **54**, 4843 (1996).
[15] A. Gupta, D. D. Awschalom, X. Peng, and A. P. Alivisatos, Phys. Rev. B **59**, R10 421 (1999).
[16] K. Leung, S. Pokrant, and K. B. Whaley, Phys. Rev. B **57**, 12 291 (1998).